0272-8842(95)00051-8

Ceramics International 22 (1996) 39–43

0272-8842/96/$15.00

Different Degradation Processes in ZnO Varistors

M. S. Castro & C. M. Aldao

Institute of Materials Science and Technology (INTEMA), Universidad Nacional de Mar del Plata, CONICET, Juan B. Justo 4302, 7600 Mar del Plata, Argentina

(Received 9 December 1994; accepted 20 April 1995)

Abstract: Degradation of ZnO-based varistors has been attributed to ion migration in the depletion layers at intergrains. Experiments can then be explained as the result of the deformation of Schottky barriers present in the grain boundaries. However, the simple lowering of the barriers is not consistent with the observed results. We found that ion migration can change the dopant profile and then the barriers' shape. We found it necessary to distinguish two processes, permanent degradation and reversible degradation to account for the observed experimental results.

1 INTRODUCTION

There has been a considerable effort to understand the degradation processes in zinc oxide varistors and their relation to microstructure.[1–7] Degradation phenomena can appear under continuous, alternating, or pulses of voltage usually combined with thermal treatments.[8,9] Suggested degradation mechanisms are electron capture, dipole orientation, ion migration and oxygen desorption. Among these, the most accepted model is due to T. K. Gupta and G. W. Carlson.[10] They propose a double barrier with a stable component consisting of spatially fixed positively charged ions and a metastable component consisting of mobile positively charged zinc interstitials. The former ions are the trivalent substitutional ions and the native oxygen vacancies, whereas the latter ions are the singly and doubly charged native zinc interstitials. The proposed degradation mechanism is based on the migration of zinc interstitials present in the depletion layers at intergrains by the action of electric fields. These ions would react at the grain boundaries with the zinc vacancies, producing a decrease in the barrier heights.

In the analysis of the electric characteristics we have used a conduction model based on a double barrier with an intergranular zone.[11] The barriers are considered to have an exponential concentration of electrically active dopants

$$N(x) = N_b + N_s \exp(-x/\lambda), \qquad (1)$$

where N_b is the donor concentration in the bulk, $N_b + N_s$ is the donor concentration in the grain boundary, and λ is a parameter.[12] Parameters N_s and λ determine the donor concentration profile close to the intergrain and thus the width and steepness of the barriers.

We found that permanent degradation can be produced by the action of a thermal treatment or by the combined action of a thermal treatment with an applied electric field. Post-sintering produces a grain growth and modifies the barriers' shape of the samples. A permanent degradation was also achieved by applying a voltage of about 30% of the breakdown voltage at 200°C.

We also found that for lower temperatures and applied voltages degradation can be reversible, that is, the varistor recovers its initial properties by relaxing at room temperature. Reversible degradation presents some difficulties in its interpretation. Although several models have been proposed to explain qualitatively what occurs in the varistor during this process, a quantitative analysis is lacking.[10]

We analyzed in this work the changes produced in ZnO-based varistors by the action of different thermal processes and applied electric fields. A model to explain the observed results is presented.

2 EXPERIMENTAL

2.1 Post-sintering

Samples were made with ZnO, 6% wt/wt Bi_2O_3, and 0·7% wt/wt MnO_2. The resulting powder was mixed and pressed at 300 kg/cm^2. Samples were then sintered at 1100°C for 3 h, cooled at 10°C/min between the sintering temperature and 700°C, and in steps of 50°C for 20 min up to 200°C. Some samples were post-sintered at 1100°C for 7 h, and cooled at 10°C/min until 700°C and then at 5°C/min until room temperature. Electric measurements were carried out in the range 80–333 K with an applied voltage of 10 V. Samples were characterized with X-ray diffraction (XRD) and Scanning Electron Microscopy (SEM).

2.2 Degradation by applying an electric field at high temperature

A commercial varistor P7 100 Z4 from General Electric was tested. Since features for varistors of the same type present varying characteristics, the same varistor was used for each measurement series. Current density–temperature characteristics (J–T curves) were determined for an applied voltage of 30 V in the range 80–463 K. Samples were then degraded by applying a voltage of 60 V at 463 K for 4 h.

2.3 Reversible degradation

In this study samples were made of ZnO with 6% wt/wt of Bi_2O_3, 0·6% wt/wt of Co_3O_4, and 3·5% wt/wt of Sb_2O_3. Current–time curves were obtained for temperatures in the range 293–413 K. Voltages lower than 70% of breakdown voltage were applied for 3 min and then the polarity was inverted. After measurements the behaviour of the varistor as-sintered was restored.

In all the degradation processes, a Phytronics power supply (0–320 V, 0–1·5 A) was used. Currents lower than 0·1 nA were measured with a home-made electrometer while a Fluke 8062A multimeter was used for higher currents. With liquid air and a furnace the desired temperatures were achieved.

3 RESULTS AND DISCUSSION

3.1 Post-sintering

The post-sintering treatment produced a high grain growth as seen in Figs 1 and 2. The same phases as those found before the treatment were detected with XRD. Electrical characteristics of the sintered and post-sintered samples are shown in Fig. 3. The post-sintering process manifests as an increase in the electrical conduction. Current density versus temperature curve fittings were achieved with following parameter values: $N_b = 7 \times 10^{16}$ cm^{-3}, $Ns = 4 \times 10^{19}$ cm^{-3}, $E_b = 1{\cdot}5$ eV, and $\lambda = 5{\cdot}1 \times 10^{-9}$ m for ZnO–Bi_2O_3 as-sintered, and $N_b = 7 \times 10^{16}$cm^{-3}, $N_s = 2 \times 10^{19}$cm^{-3}, $E_b = 1{\cdot}2$ eV and $\lambda = 6{\cdot}9 \times 10^{-9}$ m for ZnO–Bi_2O_3 post-sintered; $N_b = 7 \times 10^{16}$ cm^{-3}, $N_s = 7 \times 10^{18}$ cm^{-3}, $E_b = 1$ eV, and $\lambda = 1{\cdot}07 \times 10^{-8}$ m for ZnO–Bi_2O_3–MnO_2 as-sintered, and $N_b = 7 \times 10^{16}$ cm^{-3}, $N_s = 6 \times 10^{18}$ cm^{-3}, $E_b = 0{\cdot}95$ eV, and $\lambda = 1{\cdot}08 \times 10^{-8}$ m for ZnO–Bi_2O_3–MnO_2 post-sintered. During post-sintering (at the sintering temperature), two processes take place: an increase in the grain growth (Figs 1 and 2) due to an equivalently longer sintering time and a modification of the barriers (Fig. 3) very likely

Fig. 1. Microphotograph of the sintered varistor. Bar = 10 μm.

Fig. 2. Microphotograph of the post-sintered varistor. Bar = 10 μm.

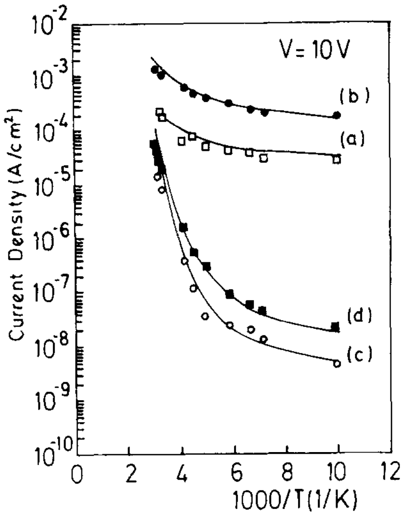

Fig. 3. Current density vs temperature curves for (a) ZnO–Bi_2O_3 as-sintered, (b) ZnO–Bi_2O_3 post-sintered, (c) ZnO–Bi_2O_3–MnO_2 as-sintered and (d) ZnO–Bi_2O_3–MnO_2 post-sintered.

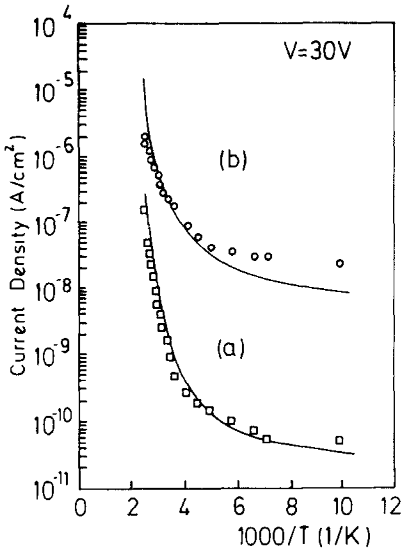

Fig. 5. Current density vs temperature for samples (a) before and (b) after degradation. As seen, a good fit cannot be obtained by changing the barrier height. $N_b = 7 \times 10^{16}\,cm^{-3}$, $N_s = 8{\cdot}7 \times 10^{18}\,cm^{-3}$, $\lambda = 1{\cdot}93 \times 10^{-8}m$, a) $E_b = 1{\cdot}52$ eV, b) $E_b = 1{\cdot}35$ eV.

produced by ion migration and loss of oxygen at the very high temperature of sintering.[13]

3.2 Degradation by applying an electric field at high temperature

Figure 4 shows that conductivity can be greatly affected by applying an electric field at high temperature. With the double barrier model described above the following parameters were determined: $N_b = 7 \times 10^{16}\,cm^{-3}$, $N_s = 8{\cdot}7 \times 10^{18}\,cm^{-3}$, $E_b = 1{\cdot}52$ eV, and $\lambda = 1{\cdot}98 \times 10^{-8}$ m before degradation, and $N_b = 7 \times 10^{16}\,cm^{-3}$, $N_s = 1 \times 10^{19}\,cm^{-3}$, $E_b = 1{\cdot}52$ eV, and $\lambda = 3{\cdot}2 \times 10^{-8}$ m after degradation. As seen, the barrier height would not be affected by this degradation process. On the other hand, dopant concentration profile at the grain boundary (parameters N_s and λ) seems to be responsible for the observed changes in the J–T curves. Figure 5 shows that a change in barrier height cannot account for the observed current–temperature curves. Barrier modification can be attributed to ion migration which modifies the donor concentration profile at the depletion regions.[13]

3.3 Reversible degradation

Figure 6 shows current evolution observed when switching the polarity of the applied voltage at different temperatures. For $T = 140°C$, a clear pattern arises in our experiments. After applying a

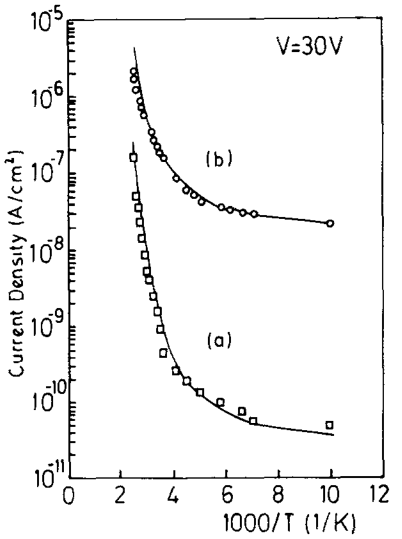

Fig. 4. Current density vs temperature for samples (a) before and (b) after degradation. As seen, a good fit is obtained without changing the barrier height.

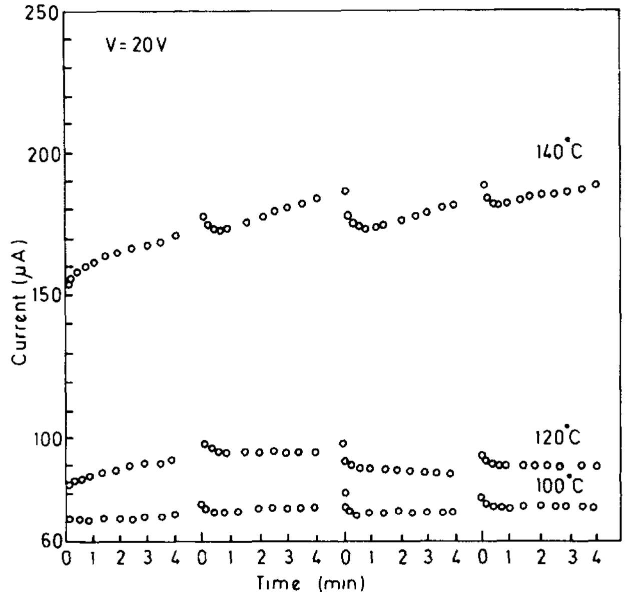

Fig. 6. Effects of switching the voltage polarity in ZnO–Bi_2O_3 samples.

voltage, the current increases with time. When the voltage polarity is inverted, the current decreases at the beginning but, after a few seconds, a steady increase is established. This behaviour appears any time the polarity is inverted. This phenomenon is not observed at low temperatures but clearly appears at temperatures above 100°C.

The transient current present after the voltage switching can be understood as the charging of the intergrain capacitances. After a few seconds, the observed trend is due to the steady-state current which directly shows the effects of degradation. This behaviour, the current magnitude, and the increase of current with time are only compatible with a fundamental change in the intergrain electrical barriers.

Reversible degradation has been explained by invoking ion diffusion in the depletion regions. Some researchers suggest that those ions are zinc interstitials which diffuse out from the depletion region to react with defects present at the grain borders.[10] This process would reduce barrier heights causing an increase of the prebreakdown current. Zn interstitials are due to the non-stoichiometric nature of ZnO frozen in their positions during cooling from the sintering temperature.

In this model, the depletion layers present fixed positive charges (oxygen vacancies), and highly mobile positive ions (zinc interstitials). This positive charge is compensated by a layer of negatively charged acceptors at the grain boundary interface (zinc vacancies). The varistor would be 'energized' during electrical stressing at temperatures high enough for ions to migrate towards the interface. These ions could then react with zinc vacancies at the grain boundary and the barrier height would decrease. When removing the applied electric field, an inverse process would take place and the barrier height would be reestablished.

When modelling the above-described mechanism by considering a field-assisted diffusion mechanism, we found that the large fields close to the grain boundaries prevents ions at the grain boundaries from migration into the grain. Indeed, it can be easily shown that ions could only penetrate a few Angstroms into the depletion layer. Since reversible stressing cycles cannot be explained by considering the positive ions' movement, we speculate that reversible stressing cycles in ZnO varistors could be a consequence of negative ions diffusing in the low-field region of the depletion layer.

4 CONCLUSIONS

From the above experimental results we found it necessary to distinguish two degradation processes: permanent and reversible degradation. Permanent degradation can be produced by the action of a post-sintering treatment causing an increase in grain sizes and changes in the barrier characteristics. Permanent degradation can also be produced when applying a not very high voltage at temperatures higher than 200°C. Reversible degradation is observed for lower applied voltages and lower temperatures. Diffusion of zinc interstitials cannot be responsible for this degradation process because of the large fields close to the grain boundaries but diffusion of other ions could be responsible for the observed results. We found that permanent and reversible degradation can be produced by changes in the shape of the intergrain barriers without invoking barrier height modifications.

REFERENCES

1. NAWATA, M., KAWAMURA, H., KANEMATSU, A. & IEDA, M., Studies on degradation mechanism of zinc oxide ceramics varistor by thermally stimulated current. In *Ceramics Transactions Vol. 3 Advances in Varistor Technology*, ed. L. M. Levinson. The American Ceramic Society, Inc., Ohio, 1989, pp. 186–93.
2. LEITE, E. R., VARELA, J. A. & LONGO, E., Barrier voltage deformation of ZnO varistors by current pulse. *J. Appl. Phys.*, **72** (1992) 147–50.
3. GUPTA, T. K., Application of zinc oxide varistors. *J. Am. Ceram. Soc.*, **73** (1990) 1817–40.
4. SATO, K., TAKADA, Y., TAKEMURA, T. & OTOKAKE, M., Carrier trapping model of degradation in ZnO varistor. In *Advances in Ceramics Vol. 7, Additives and Interfaces in Electronic Ceramics*, ed. M. F. Yan & A. H. Heuer. The American Ceramic Society, Inc., Ohio, 1982, pp. 22–9.
5. GUPTA, T. K. & CARLSON, G. W., Defect-induced degradation of barrier in ZnO varistor. In *Advances in Ceramics Vol. 7, Additives and Interfaces in Electronic Ceramics*. ed. M. F. Yan & A. H. Heuer. The American Ceramic Society, Inc., Ohio, 1982, pp. 30–40.
6. SEITZ, M. A., HAMPTON, F. & RICHMOND, W. C., Influence of chemisorbed oxygen on the ac electrical behavior of polycrystalline ZnO. In *Advances in Ceramics Vol. 7, Additives and Interfaces in Electronic Ceramics*, ed. M. F. Yan & A. H. Heuer. The American Ceramic Society, Inc., Ohio, 1982, pp. 60–70.
7. OLSSON, E., Interfacial microstructure in ZnO varistor materials. Doctoral thesis, Goteborg, 1988.
8. PHILIPP, H. R. & LEVINSON, L. M., Degradation phenomena in zinc oxide varistors: a review. In *Advances in Ceramics Vol. 7, Additives and Interfaces in Electronic Ceramics*, ed. M. F. Yan & A. H. Heuer. The American Ceramic Society, Inc., Ohio, 1982, pp. 1–21.
9. SONDER, E., AUSTIN, M. M. & KINSER, D. L., Effect of oxidizing and reducing atmospheres at elevated temperatures on the electrical properties of zinc oxide varistors. *J. Appl. Phys.*, **54** (1983) 3566–72.
10. GUPTA, T. K. & CARLSON, G. W., A grain-boundary defect model for instability/stability of ZnO varistor. *J. Mater. Sci.*, **20** (1985) 3487–500.

11. CASTRO, M. S. & ALDAO, C. M., Prebreakdown conduction in zinc oxide varistors: thermionic or tunnel currents and one-step or two-step conduction processes. *Appl. Phys. Lett.*, **63** (1993) 1077–9.
12. CASTRO, M. S., PERISSINOTTI, L. & ALDAO C. M., Cooling rate effects in ZnO varistors. *J. Mater. Sci.: Mat. in Electronics*, **3** (1992) 218–21.
13. LEITE, E. R., VARELA, J. A. & LONGO, E., A new interpretation for the degradation phenomenon of ZnO varistors. *J. Mater. Sci.*, **27** (1992) 5325–9